

Inhibitors

International Edition: DOI: 10.1002/anie.201608672
German Edition: DOI: 10.1002/ange.201608672

Azaindoles as Zinc-Binding Small-Molecule Inhibitors of the JAMM Protease CSN5

Eva Altmann,* Paul Erbel, Martin Renatus, Michael Schaefer, Anita Schlierf, Adelaide Druet, Laurence Kieffer, Mickael Sorge, Keith Pfister, Ulrich Hassiepen, Matthew Jones, Simon Ruedisser, Daniela Ostermeier, Bruno Martoglio, Anne B. Jefferson, and Jean Quancard

Abstract: CSN5 is the zinc metalloprotease subunit of the COP9 signalosome (CSN), which is an important regulator of cullin-RING E3 ubiquitin ligases (CRLs). CSN5 is responsible for the cleavage of NEDD8 from CRLs, and blocking deconjugation of NEDD8 traps the CRLs in a hyperactive state, thereby leading to auto-ubiquitination and ultimately degradation of the substrate recognition subunits. Herein, we describe the discovery of azaindoles as a new class of CSN5 inhibitors, which interact with the active-site zinc ion of CSN5 through an unprecedented binding mode. The best compounds inhibited CSN5 with nanomolar potency, led to degradation of the substrate recognition subunit Skp2 in cells, and reduced the viability of HCT116 cells.

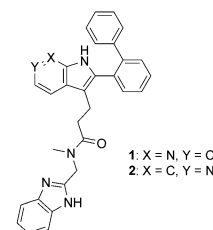
Cullin-RING ligases (CRLs) represent the largest family of E3 ubiquitin ligases, which are responsible for about 20% of total cellular protein turnover through the ubiquitin-proteasome system.^[1] Neddylation and deneddylation of CRLs are integral steps in their assembly as active complexes, regulating binding and ubiquitination of proteins during cell-cycle progression, cell growth, and survival. Deneddylation, an essential step for maintaining optimal levels of CRL activity,^[2] is mediated by the COP9 signalosome (CSN), a protein complex comprising eight subunits.^[3] The deneddylation of CRLs is required for new substrate binding and to prevent autoubiquitination and subsequent degradation of the substrate recognition subunits of the CRL.^[4] The subunit CSN5, a JAMM metalloprotease, is responsible for the cleavage of ubiquitin-like NEDD8 from CRLs. Importantly, CSN5

requires the structural CSN framework for exerting isopeptidase activity.^[5] Elevated expression of CSN5 has been found in breast, thyroid, skin, ovarian, lung, and liver cancers.^[6] In hepatocellular carcinoma cells, knockdown of CSN5 by small-interfering RNA (siRNA) inhibits cell-cycle progression and causes strong induction of apoptosis in vitro.^[7] The down-regulation of CSN5 impedes CSN function, as demonstrated by an accumulation of neddylated cullin 1 (Cul1), and results in a decrease in the oncogenic F-box protein Skp2. Stabilization of the NEDD8–CRL complex through inhibition of CSN5 could thus represent a novel therapeutic approach for the treatment of CSN5-dependent cancers.^[8,9]

A high-throughput screening of the entire Novartis compound archive was carried out using a time-resolved fluorescence energy transfer (TR-FRET)-based protease activity assay with recombinant CSN and a fluorescence-labelled NEDD8-modified CRL as a substrate (Table S1 in the Supporting Information). Among other hits^[10] a series of 7-azaindoles, exemplified by compound **1**, were identified as CSN5 inhibitors. In a dose–response experiment, the half maximal inhibitory concentration (IC₅₀) of **1** was determined to be 1.4 μM in a fluorescence polarization (FP)-based protease activity assay.^[11] To further validate **1** as a CSN5 inhibitor, we performed binding studies with recombinant CSN5(2-257).

Even though the isolated enzyme is not proteolytically active, we speculated that the compound could still bind to the protein, since the active site is largely intact.^[12] In addition, we demonstrated that the isolated protein is capable of binding zinc, as shown by the 8°C increase in the melting temperature of recombinant CSN5(2-257) when Zn²⁺ is added (Figure S1 in the Supporting Information). We measured affinity by surface plasmon resonance (SPR) and found that **1** bound reversibly to CSN5(2-257) with a K_D value of 1.5 μM, which is in line with its potency in the biochemical assay (Figure 1 A).

We then used nuclear magnetic resonance (NMR) spectroscopy to further characterize the binding of **1** to CSN5(2-257). As shown in Figure 2, in the absence of ligand, the resonances of two methionines (ε methyl group) are very weak and broadened to dynamics. Addition of compound **1** to the protein leads to chemical-shift changes and an intensity increase of these methyl signals. Selective ¹³C labelling of methionine residues combined with site-directed mutagenesis



[*] Dr. E. Altmann, Dr. P. Erbel, Dr. M. Renatus, Dr. M. Schaefer, Dr. A. Schlierf, A. Druet, L. Kieffer, M. Sorge, K. Pfister, Dr. U. Hassiepen, M. Jones, Dr. S. Ruedisser, D. Ostermeier, Dr. B. Martoglio, Dr. J. Quancard
Novartis Institutes for BioMedical Research
Novartis Campus, 4002 Basel (Switzerland)
E-mail: eva.altmann@novartis.com

K. Pfister, Dr. A. B. Jefferson
Novartis Institutes for BioMedical Research
4560 Horton Street, Emeryville, CA 94608-2916 (USA)

Dr. B. Martoglio
Present address: Pharma Research and Early Development
Roche Innovation Center Basel, 4070 Basel (Switzerland)

Dr. A. B. Jefferson
Present address: Centers for Therapeutic Innovation, Pfizer Inc.
San Francisco, CA 94158 (USA)

Supporting information and the ORCID identification number(s) for the author(s) of this article can be found under <http://dx.doi.org/10.1002/anie.201608672>.

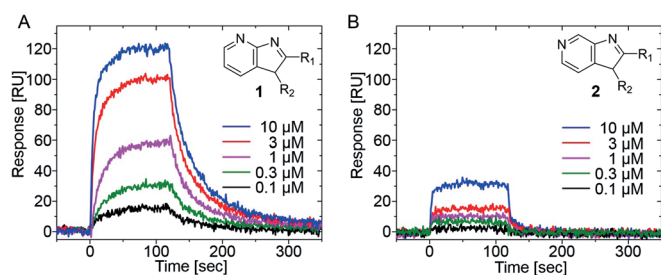


Figure 1. SPR sensograms for the binding of 7-azaindole **1** (A) and 6-azaindole **2** (B) to CSN5, as measured on a ProteOn GLM sensor chip coated with CSN5 to a value of 120 RU. The same compound dilution range (10, 3, 1, 0.3, 0.1 μM) was used in both experiments. The data demonstrate binding of **1** to CSN5, while no binding is observed for **2**.

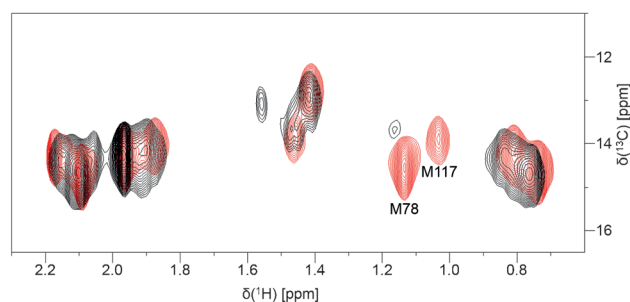


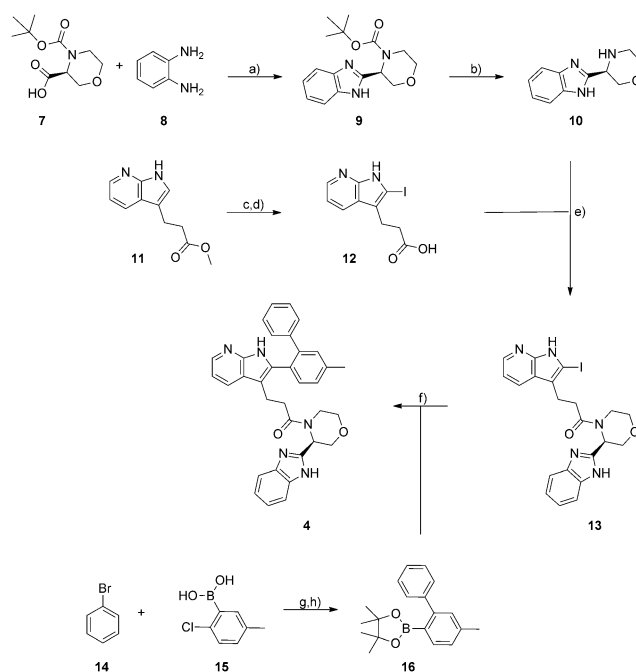
Figure 2. HSQC of ^{13}C -methionine-labelled CSN5(2-257) in the absence (black) and presence (red) of compound **1**. The HSQC experiment was performed at a concentration of 40 μM CSN5(2-257) and 200 μM of compound **1**.

(see the Supporting Information) and information from a preliminary, low-resolution structure of CSN5(2-257) allowed us to assign the methyl resonances of M78, which is in close proximity to the active-site zinc, and of M117, which is part of the flexible α -helical loop region covering the substrate binding cleft.

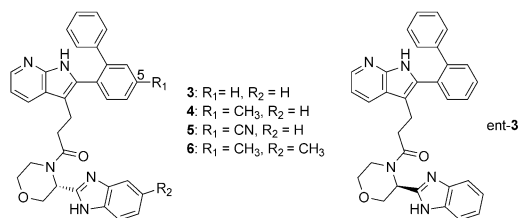
The data suggest that inhibitor **1** targets the CSN5 catalytic site. Surprisingly, compound **1** does not contain any known Zn^{2+} binding motif,^[13] which raised the question of its mode of action. The close analogue **2**, which contains a 6-azaindole motif, did not inhibit the enzyme and was shown by SPR not to bind to CSN5 (Figure 1B). This suggests that the 7-azaindole substructure is essential for binding.

Initial co-crystallization trials of **1** with CSN5(2-257) were unsuccessful, possibly due to the moderate binding affinity of the compound. We thus engaged in an optimization effort focusing on improving biochemical potency. Key compounds **3–6** and *ent-3* were prepared in the course of this optimization. The synthesis of these new azaindole inhibitors followed the route exemplified for compound **4** in Scheme 1.

Coupling of Boc-morpholine-(*S*)-3-carboxylic acid **7** with diamine **8** using HBTU afforded an amide intermediate that was dehydrated at elevated temperatures to afford benzimidazole **9** (Scheme 1). Boc removal with HCl/dioxane yielded intermediate **10**. Silver triflate assisted C2-iodination of azaindole **11** provided methyl 3-(2-iodo-1-*H*-pyrrolo[2,3-*b*]pyridin-3-yl)propanoate, which was hydrolyzed with LiOH to the corresponding acid **12**. In the following step,



Scheme 1. a) i. HATU, DMF, RT; ii. AcOH, 70 $^{\circ}\text{C}$, 80%. b) 4 M HCl in dioxane, RT, 98%. c) I_2 , $\text{CF}_3\text{SO}_3\text{Ag}$, THF, RT, 54%. d) LiOH, THF/ H_2O (3:1), RT, 96%. e) HBTU, DIEA, DMF, RT, 91%. f) $\text{Pd}(\text{PPh}_3)_2\text{Cl}_2$, Na_2CO_3 , DME, 90 $^{\circ}\text{C}$, 11%. g) $\text{Pd}(\text{PPh}_3)_2\text{Cl}_2$, Na_2CO_3 , DME, 90 $^{\circ}\text{C}$, 96%. h) Bis(pinacolato)diboron, $\text{Pd}_2(\text{dba})_3$, XPhos, KOAc, dioxane/ H_2O (2:1), 110 $^{\circ}\text{C}$, 69%. For details see the Supporting Information. HATU = *N*-[(dimethylamino)-1-*H*-1,2,3-triazolo-[4,5-*b*]pyridin-1-ylmethyl]-*N*-methylmethanaminium hexafluorophosphate *N*-oxide, THF = tetrahydrofuran, HBTU = *N,N,N',N'*-tetramethyl-*O*-(1-*H*-benzotriazol-1-yl)uronium hexafluorophosphate, DIEA = *N*-ethyl-diisopropylamine, DMF = *N,N*-dimethylformamide, DME = 1,2-dimethoxyethane, 1,2-dimethoxyethane.



intermediate **12** was coupled to the morpholino-benzimidazole **10** to give **13**. Elaboration of **13** to target molecule **4** was accomplished through a palladium(0)-catalyzed arylation with **16**.

We were able to solve an X-ray co-crystal structure of inhibitor **4** in complex with CSN5(2-257) at a resolution of 2.2 \AA (Figure 3) and refine it to an R_{free} of 21.9% (Table S3). The structure shows that the compound is bound in the active site of the enzyme and displays an unprecedented binding mode for a zinc metalloprotease inhibitor. The azaindole moiety is bound in the catalytic center of CSN5 through a dual interaction. N7 coordinates to the active-site Zn^{2+} ($\text{N}-\text{Zn}$ distance of 2.1 \AA) in a monodentate fashion, while the NH forms a tight hydrogen bond with O_γ of the D151 carboxylate (Figure 3C). The proximal 5-methyl-phenyl group of the 2-

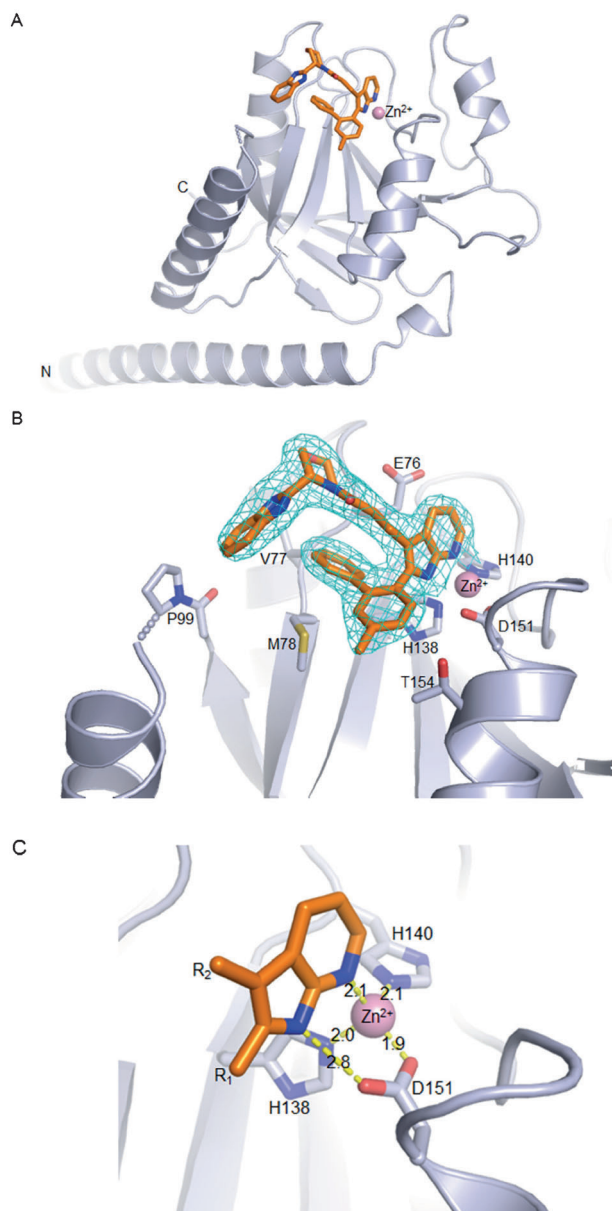


Figure 3. X-ray co-crystal structure of **4** (orange) bound in the active site of CSN5 (2-257) (gray) at 2.2 Å resolution (PDB ID: 5M5Q), refined to R_{free} of 21.9%. A) Overall structure as a cartoon representation with the ligand shown as a stick representation. The N and C termini of the polypeptide chain are indicated. B) The cyan mesh represents the refined $2F_o - F_c$ electron density map (contoured at 1σ). The dotted line depicts a stretch of amino acids (100–108) that are poorly defined by electron density and were removed from the final model. C) A detailed interaction pattern for the azaindole core with the active site Zn^{2+} ion and D151. Distances are given in Å. All images were generated using PyMOL (The PyMOL Molecular Graphics System, Version 1.8.2.2, Schrödinger, LLC).

biphenyl substituent fills a lipophilic pocket formed by V77 and T154, whereas the distal phenyl ring is orientated towards a lipophilic cavity formed by M78 and V77. The spacer and the morpholino group position the benzimidazole substituent in a hydrophobic area around P99. The benzimidazole group and the distal phenyl ring of the biphenyl moiety are involved

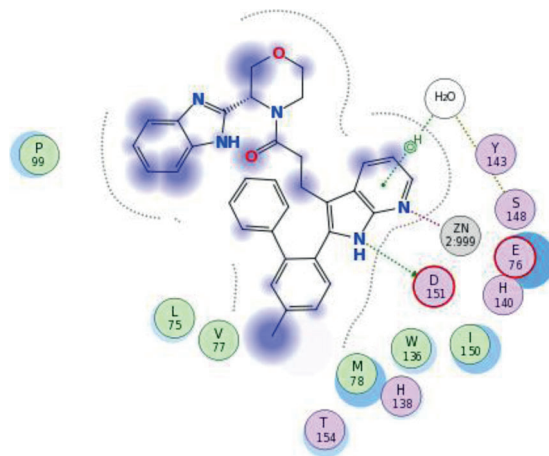


Figure 4. A ligand-interaction diagram for ligand **4**. The ligand-interaction plot was generated using the algorithm described by Clark et al.^[14].

in an intramolecular edge-to-face stacking interaction (Figure 4).

The inhibitory activity of azaindole derivatives **3–6** was determined in a FP-based protease activity assay with recombinant CSN holoenzyme and PT22-Nedd8-Cul4 as the substrate. IC_{50} values for the inhibition of CSN5, as determined in this assay, are reported in Table 1. A clear improve-

Table 1: Activities of the 7-azaindole derivatives.

Compound	1	3	ent-3	4	5	6
IC_{50} [μM] ^[a]	1.4	0.1	1.2	0.09	0.18	0.06

[a] Inhibition of CSN5 in a FP-based protease activity assay using PT22-Nedd8-Cul4 as substrate. Data represent the mean of at least 2 experiments performed in duplicate. Individual data points were within a 2-fold range with each other. For details, see the Supporting Information.

ment in potency to an IC_{50} of 0.1 μM was achieved through rigidification of the linker moiety. The rigidification was attained by making the bond connecting the amide nitrogen to the benzimidazole moiety part of a morpholine ring (Table 1, compound **3**). Specific inhibition of CSN protease activity by **3** was also confirmed by the 12-fold lower potency of its enantiomer *ent*-**3**. Based on the structure of the morpholino analogue **3**, the effects of attaching small peripheral substituents were evaluated. Only moderate changes in potency were observed for most substituents investigated, for example, a methyl (**4**) or cyano (**5**) substituent at position 5 of the proximal phenyl ring. A slight improvement in potency relative to **3** was observed with the doubly methylated compound **6**.

We next explored the specificity profiles of compounds **4** and **6** against a panel of seven human matrix metalloproteases (MMPs; Table S2). None of the MMPs tested was inhibited significantly by these compounds. It could be that the different active-site architectures of MMPs^[15] compared to CSN5, namely the coordination of the Zn^{2+} , disfavors binding

of the azaindole moiety. As shown in Figure 3C, D151, the third zinc-coordinating residue in CSN5, plays a key role in ligand binding and is involved in a hydrogen-bonding interaction with the NH of the azaindole. In contrast to JAMM proteases, where the catalytic zinc is coordinated by two histidines and one aspartate (H138, H140, D151), the catalytic zinc ion in MMPs is coordinated by three histidine residues. Consequently, binding interactions with the 6-azaindole motif are not possible, and in addition, there is not enough space to accommodate the bicyclic heterocyclic core in the MMP active site.

We then assessed the effects of our inhibitors in cellular systems. Treatment of human colon carcinoma derived HCT116 cells with inhibitors **5** or **6** led to the trapping of Cul1 in the neddylated state (Figure 5A), thus demonstrating inhibition of deneddylation. As a consequence, the oncogenic F-box protein Skp2 was degraded in a dose-dependent manner. These results mirror the effects observed when CSN5 is depleted by siRNA.^[7] Next we explored the effect of these inhibitors on the viability of HCT116 cells. Compounds **5** and **6** exhibited potent inhibition of proliferation, as seen in a CellTiter-Glo assay, with EC₅₀ values of 4.7 and 4.9 μM , respectively, which confirms the potential of CSN5 inhibitors as anticancer agents (Figure 5B).

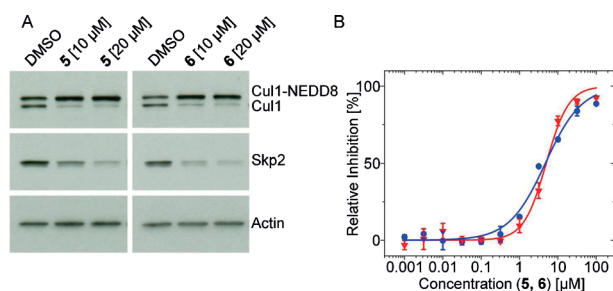


Figure 5. A) Biological effects of the CSN5 inhibitors. An immunoblot is shown for Cul1 and Skp2 after treatment of HCT116 cells with compounds **5** and **6** at the indicated concentrations. B) Inhibition of cell proliferation with CSN5 inhibitors **5** and **6**. Individual dose-response curves for HCT116 cells treated with **5** (blue points) and **6** (red triangles), $n=2$, results are shown as the mean \pm SD. The experimental data were fitted using the nonlinear regression program Origin 8.5.0 SR1 (OriginLab Corporation, Northampton, MA). For details, see the Supporting Information.

In summary we have discovered a novel class of active-site-directed, small-molecule inhibitors of the JAMM protease CSN5. The X-ray co-crystal structure of one these compounds with CSN5 revealed an unprecedented binding mode, with the 7-azaindole core coordinating the active-site Zn^{2+} ion through N7, and the indole NH engaging in a hydrogen bond with the D151 side-chain carboxylate. The optimized inhibitors are selective for CSN5 over other human metalloproteases. They recapitulate the effects observed for CSN5 knockdown by siRNA and they inhibit cell prolifer-

ation in HCT116 cells. While further improvements in potency are still required to reach a suitable drug candidate, our study, provides an important proof-of-concept for the usefulness of CSN5 inhibitors as anticancer agents.

Keywords: azaindoles · CSN5 · ubiquitin ligases · inhibitors · metalloproteases

- [1] a) M. D. Petroski, R. J. Deshaies, *Nat. Rev. Mol. Cell Biol.* **2005**, 6, 9; b) R. J. Deshaies, C. A. Joazeiro, *Annu. Rev. Biochem.* **2009**, 78, 399.
- [2] N. W. Pierce, J. E. Lee, X. Liu, M. J. Sweredoski, R. L. J. Graham, E. A. Larimore, M. Rome, N. Zheng, B. E. Clurman, S. Hess, S. Shan, R. J. Deshaies, *Cell* **2014**, 153, 161.
- [3] G. M. Lingaraju, R. D. Bunker, S. Cavadini, D. Hess, U. Hassiepen, M. Renatus, E. S. Fischer, N. H. Thomä, *Nature* **2014**, 512, 161.
- [4] a) G. A. Cope, R. J. Deshaies, *BMC Biochem.* **2006**, 7, 1; b) R. J. Deshaies, E. D. Emberley, A. Saha, *Subcell. Biochem.* **2010**, 54, 41; c) T. Schmalzer, W. Dubiel, in *Conjugation and deconjugation of ubiquitin family modifiers* (Ed: M. Groettrup), Springer, New York, **2010**, pp. 57–68; d) D. M. Duda, D. C. Scott, M. F. Calabrese, E. S. Zimmerman, N. Zheng, B. A. Schulman, *Curr. Opin. Struct. Biol.* **2011**, 21, 257; e) E. D. Emberley, R. Mosadeghi, R. J. Deshaies, *Biol. Chem.* **2012**, 287, 29679.
- [5] A. Echalié, Y. Pan, M. Birol, N. Tarvernier, L. Pintard, F. Hoh, C. Ebel, N. Galophe, F. X. Claret, C. Dumas, *Proc. Natl. Acad. Sci. USA* **2013**, 110, 1273.
- [6] a) M.-H. Lee, R. Zhao, L. Phan, S.-C. J. Yeung, *Cell Cycle* **2011**, 10, 3057.
- [7] Y.-H. Lee, A. D. Judge, D. Seo, M. Kitade, L. E. Gomez-Quiroz, T. Ishikawa, J. B. Andersen, B.-K. Kim, J. U. Marquardt, C. Raggi, I. Avital, E. A. Conner, I. MacLachlan, V. M. Factor, S. S. Thorgeirsson, *Oncogene* **2011**, 30, 4175.
- [8] T. J. Shackleford, F. X. Claret, *Cell Div.* **2010**, 5, 26.
- [9] J. R. Skaar, J. K. Pagan, M. Pagano, *Nat. Rev. Drug Discovery* **2014**, 13, 889.
- [10] A. Schlierf, E. Altmann, J. Quancard, A. B. Jefferson, R. Assenberg, M. Renatus, M. Jones, U. Hassiepen, M. Schaefer, M. Kiffe, A. Weiss, C. Wiesmann, R. Sedrani, J. Eder, B. Martoglio, *Nat. Commun.* **2016**, 7, 13166.
- [11] J. R. Lakowicz, *Principles of Fluorescence Spectroscopy*, Springer, New York, **2006**, p. 1.
- [12] S. Cavadini, E. S. Fischer, R. D. Bunker, A. Potenza, G. M. Lingaraju, K. N. Goldie, W. I. Mohamed, M. Faty, G. Petzold, R. E. J. Beckwith, R. B. Tichkule, U. Hassiepen, W. Abdulrahman, R. S. Pantelic, S. Matsumoto, K. Sugawara, H. Stahlberg, N. H. Thomä, *Nature* **2016**, 531, 598.
- [13] K. Kawai, N. Nagata, *Eur. J. Med. Chem.* **2012**, 51, 271.
- [14] A. M. Clark, P. Labute, M. Santavy, *J. Chem. Inf. Model.* **2006**, 46, 1107.
- [15] C. Tallant, A. Marrero, F. X. Gomis-Rüth, *Biochem. Biophys. Acta Mol. Cell Res.* **2010**, 1803, 20.

Manuscript received: September 5, 2016

Revised: October 27, 2016

Final Article published: ■ ■ ■ ■ ■ ■ ■ ■ ■ ■

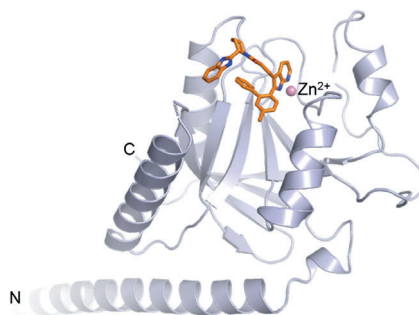
Communications



Inhibitors

E. Altmann,* P. Erbel, M. Renatus,
M. Schaefer, A. Schlierf, A. Druet,
L. Kieffer, M. Sorge, K. Pfister,
U. Hassiepen, M. Jones, S. Ruedisser,
D. Ostermeier, B. Martoglio,
A. B. Jefferson,
J. Quancard ————— ■■■■-■■■■

Azaindoles as Zinc-Binding Small-
Molecule Inhibitors of the JAMM
Protease CSN5



CSN5 is the zinc metalloprotease subunit of the COP9 signalosome, which is an important regulator of cullin-RING E3 ubiquitin ligases. A new class of CSN5 inhibitors (orange) was discovered and shown to interact with the active-site zinc ion in an unprecedented binding mode. Optimized nanomolar CSN5 inhibitors result in decreased levels of the onco-protein Skp2 and reduce the viability of HCT116 cells.